

0 0 0 0 4 4 0 5 8 5 3

*Presented at the Second International  
Symposium on Land Subsidence,  
Anaheim, CA, December 10-17, 1976*

LBL-4461  
c.1

RECEIVED  
LAWRENCE  
BERKELEY LABORATORY

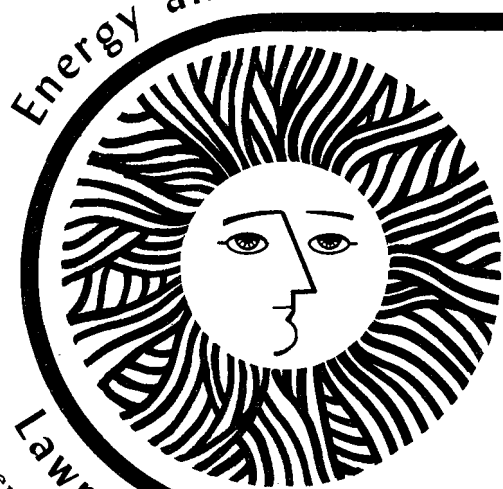
MAR 9 1977

LIBRARY AND  
DOCUMENTS SECTION

## For Reference

Not to be taken from this room

Energy and Environment Division



### Numerical Model for Land Subsidence in Shallow Groundwater Systems

*T. N. Narasimhan and  
P. A. Witherspoon*

December 1976

Lawrence Berkeley Laboratory University of California/Berkeley  
Prepared for the U.S. Energy Research and Development Administration under Contract No. W-7405-ENG-48

LBL-4461  
c.1

**LEGAL NOTICE**

*This report was prepared as an account of work sponsored by the United States Government. Neither the United States nor the United States Energy Research and Development Administration, nor any of their employees, nor any of their contractors, subcontractors, or their employees, makes any warranty, express or implied, or assumes any legal liability or responsibility for the accuracy, completeness or usefulness of any information, apparatus, product or process disclosed, or represents that its use would not infringe privately owned rights.*

0 0 0 0 4 4 0 5 8 5 4

NUMERICAL MODEL FOR LAND SUBSIDENCE IN SHALLOW GROUNDWATER SYSTEMS

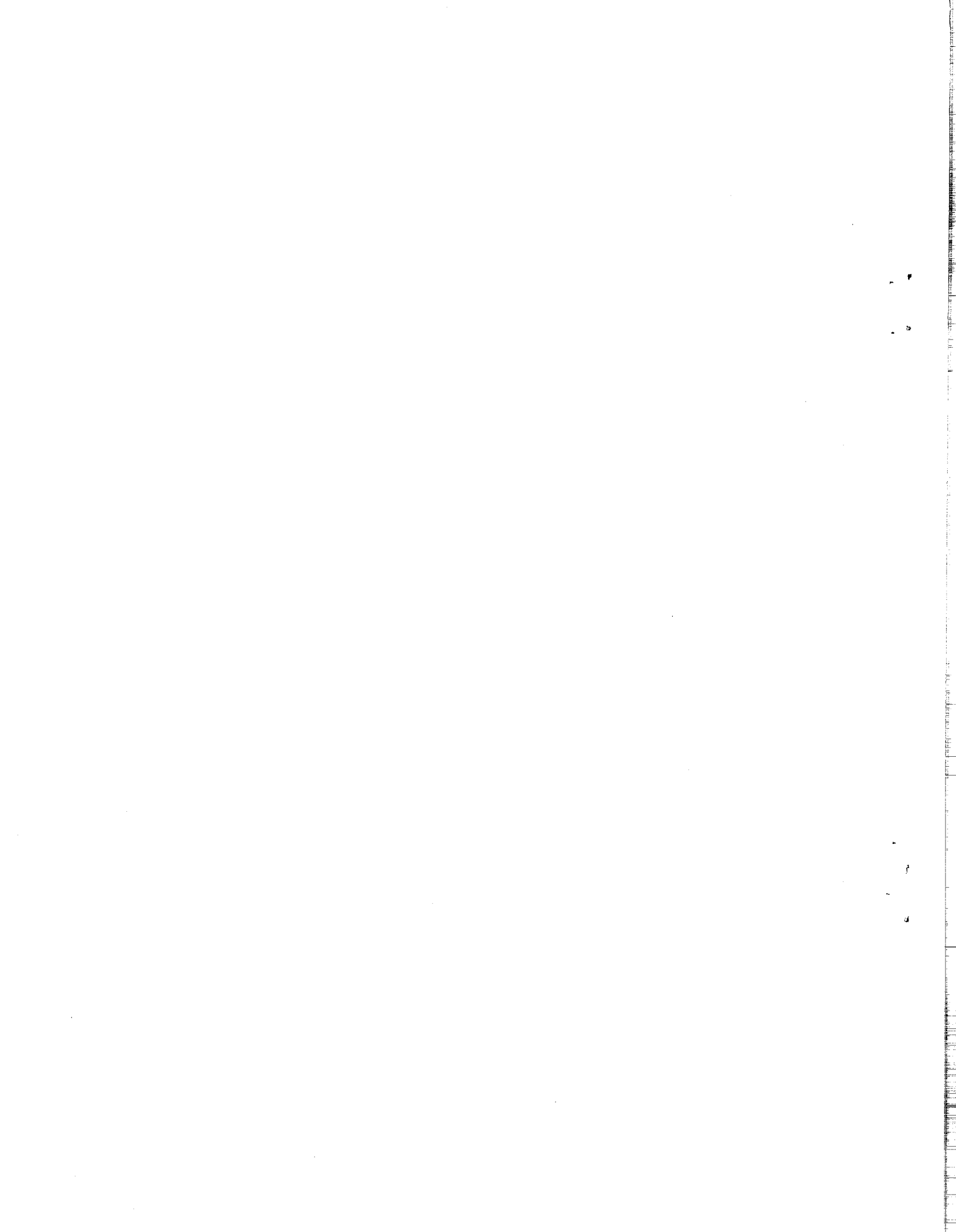
by

T. N. Narasimhan and P. A. Witherspoon  
Lawrence Berkeley Laboratory  
and  
Department of Materials Science and Engineering  
University of California  
Berkeley, California 94720

December 1976

Presented at the  
Second International Symposium on Land Subsidence  
Anaheim, California, December 10-17, 1976

This work was supported in part by the U. S. Energy  
Research and Development Administration



## NUMERICAL MODEL FOR LAND SUBSIDENCE IN SHALLOW GROUNDWATER SYSTEMS

T. N. Narasimhan and P. A. Witherspoon

Lawrence Berkeley Laboratory and Department of Materials Science & Engineering  
University of California  
Berkeley, California 94720Abstract

A numerical model is presented to simulate compaction of shallow groundwater systems. The model combines a general three-dimensional fluid flow field with a one-dimensional deformation of the porous medium. The governing equation is solved with an Integrated Finite Difference Method using a mixed explicit-implicit iteration scheme for advancing in the time domain. The model can handle heterogeneous flow regions with complex geometry, and with time dependent variation of material properties and boundary conditions. Five illustrative examples are provided to demonstrate the applicability of the model to problems of relevance in studying land subsidence.

Introduction

The purpose of this paper is to present a numerical model for simulating the compaction of a groundwater reservoir caused by withdrawal of water. As used here, the term groundwater reservoir includes those parts of the groundwater system which release water from storage in order to directly compensate for the water withdrawn. If the reservoir occurs at a shallow depth, all the deformations associated with the compaction may be expressed at ground surface as land subsidence. If the reservoir is buried at considerable depths, the effects of compaction may undergo more or less attenuation in being transmitted to the land surface through the overburden. The propagation of the effects of reservoir compaction through the overburden is outside the scope of this paper. Conceptually, the model combines a general three-dimensional fluid flow field with a one-dimensional, vertical, deformation of the porous medium. The first part of the paper deals with the theory and the salient features of the model. In the second, five illustrative examples are given to demonstrate the applicability of the model to problems that are relevant in studying land subsidence.

Theory

The equation governing saturated-unsaturated flow in a deforming porous medium can be expressed in an integral form as (Narasimhan and Witherspoon, 1976b)

$$G + \int_{\Gamma} \bar{\rho}_w \bar{k} \nabla(z+\psi) \cdot \vec{n} \, d\Gamma = M_c \frac{D\psi}{Dt} \quad (1)$$

in which  $\Gamma$  is the surface of an appropriately small volume element fixed in the solid phase of the porous medium,  $D/Dt$  is a material derivative and  $M_c$ , the fluid mass capacity of the volume element defined by

$$M_c = V_s \rho_w \left[ \underbrace{e S_w \beta}_{\text{expansion of water}} + \underbrace{S_w \chi' a_v}_{\text{change in pore volume}} + \underbrace{e \frac{dS}{d\psi}}_{\text{change in saturation}} \right] \quad (2)$$

$M_c$  denotes the mass of water which the volume element can release from storage due to an unit change in the mean value of  $\psi$ .

Restricting ourselves, in this paper, to a saturated flow region and neglecting small changes in  $\rho_w$ , (1) reduces to

$$G + \int_{\Gamma} \rho_{w0} \bar{K} \nabla(z+\psi) \cdot \vec{n} \, d\Gamma = \rho_{w0} V_s \gamma_w [e\beta + \chi' a_v] \frac{D\psi}{Dt} \quad (3)$$

As opposed to (3) it is more customary in hydrogeology literature to write the governing equation in the form

$$G + \int_{\Gamma} \rho_{w0} \bar{K} \nabla(z+\psi) \cdot \vec{n} \, d\Gamma = \rho_{w0} V \gamma_w [n\beta + m_v] \frac{\partial \psi}{\partial t} \quad (4)$$

The quantity,  $\gamma_w [n\beta + m_v]$  is often referred to as specific storage,  $S_s$ .

In dealing with reservoir compaction, the treatment of the deformation parameter is critical. As pointed out by Helm [1974], it is necessary to distinguish between recoverable (elastic) and non-recoverable (non-elastic, virgin) components of compaction. This distinction can be implemented in the present model by using different values of  $a_v$  (in equation 3) or  $S_s$  (in equation 4) for the elastic and virgin compression ranges. Alternatively, one could replace  $a_v$  in (3) by  $c_c/\sigma'$  or  $c_s/\sigma'$ .

The governing equations (3) and (4) are subject to appropriate initial and boundary conditions. The equations are in general non-linear since  $K$  and  $M_c$  are both functions of the dependent variable  $\psi$ . To numerically solve the equations, an Integrated Finite Difference Method (Narasimhan and Witherspoon, 1976a) has been employed, using a mixed explicit-implicit iterative procedure to advance in time. The details of the algorithm can be found in Narasimhan (1975) and will be published elsewhere.

In general, the model can simulate a heterogeneous three dimensional flow region with complex geometry. Anisotropy can be taken into account by orienting the elemental interfaces normal to the principal axes of anisotropy. The source term as well as the boundary condition can be dependent on time or on  $\psi$ . The total stress may be prescribed to vary with time. The initial state of  $\psi$  and preconsolidation stress may be arbitrary. The material properties,  $K$ ,  $e$ ,  $a_v$ ,  $m_v$ ,  $n$  and  $S_s$  may vary with effective stress. A choice is available either to use (3) or (4) as the governing equation, although, (3) is technically preferable, especially when the material properties are stress dependent.

Probably the chief limitation of the model is that it ignores lateral deformations. For hydrogeological systems with large lateral dimensions, ignoring lateral deformations appears to be valid in the light of the recent work by Helm (1975). Perhaps the only way to realistically simulate lateral displacements is to solve a second governing equation for stress-strain, suitably coupled with the flow equation (3). This necessarily leads to increased effort and increased requirement of refined field data. Such a coupled model may be especially needed if there is a significant overburden between the reservoir and the land surface.

#### Illustrative Examples

In order to verify the model, the five problems listed below were solved:

1. One-dimensional, homogeneous clay column. Step-change in total stress, followed by drainage.
2. One-dimensional, heterogeneous clay, column. Step-change in total stress, followed by drainage.
3. One-dimensional, homogeneous clay column. Constant total stress. Cyclic variation of hydraulic head at the boundary.
4. Two-dimensional, homogeneous region. Time-dependent total stress with drainage.

5. Axi-symmetric, leaky aquifer system. Constant total stress. Pumpage from a well.

Example 1. There are 100 doubly-draining beds of clay, normally consolidated and under hydrostatic conditions. At  $t = 0$  a step-load equal to 3.05 m of water is applied at the boundary of each bed, resulting in the development of 3.05 m of excess pore-pressure within each-bed. The clay has  $K' = 9.67 \times 10^{-12}$  m/sec and  $S_s = 3.28 \times 10^{-4} \text{ m}^{-1}$ . It is required to compute total compaction as a function of time. The problem was solved numerically using a mesh spacing of  $6.096 \times 10^{-2}$  m. An analytic solution for the problem can be found in Taylor (1948). A comparison of the analytical and the numerical solutions show excellent agreement (Figure 1).

Example 2. Schiffman and Gibson (1964) reasoned that for realistic settlement calculations due consideration must be given to the variability of permeability and compressibility with depth in thick clay columns. To establish their hypothesis, they considered a 30.48 m column of London Blue clay (Figure 2) with depth-dependent material properties (Figure 3). Treating  $K$  and  $m_v$  as continuous functions of depth and using a finite difference model they computed compaction as a function of time. The same problem was solved by our numerical model, by dividing the column into 10 materials with step-wise change in properties (Figure 3) and 100 volume elements. A comparison of the results is shown in Figure 4. The agreement appears reasonable and the small differences seen after two years is probably attributable to the different techniques employed for handling the spatial variation of material properties.

Example 3. The subsidence of land surface as well as the associated fluctuation in piezometric heads near Pixley, California has been carefully measured over several years by the U. S. Geological Survey (Lofgren and Klausning, 1969). Recently, Helm (1975) successfully modeled observed subsidence at Pixley for a 12-year period from 1958, treating the observed piezometric fluctuations as the causative mechanism. Within the alluvial sediments at Pixley there exist 21 compacting clay beds of varying thickness, aggregating 85 m and separated by hydraulically continuous, highly permeable sand beds. In accordance with Helm's findings, the Pixley system was treated in the present study as equivalent to 17 doubly draining clay beds, each 4.877 m thick. Because of symmetry, only one half of a bed need be modeled. The column was discretized into 20 elements, 0.1219 m thick. The following material properties were used:  $K' = 2.9 \times 10^{-11}$  m/sec;  $(S_s)_{\text{virgin}} = 7.54 \times 10^{-4} \text{ m}^{-1}$ ;  $(S_s)_{\text{elastic}} = 1.51 \times 10^{-5} \text{ m}^{-1}$ . The boundary conditions consisted of day by day hydrographs of the piezometric variations in the aquifer. The simulation was carried out for 4000 days from October 21, 1958. The initial distribution of pore pressure was assumed hydrostatic while that of the preconsolidation stress was assumed to vary parabolically from the bottom to the center of the clay bed.

A comparison between the observed and computed compactations presented in Figure 5 shows a reasonable agreement, with a maximum deviation of about 7 percent in early 1964. A similar accuracy was also obtained by Helm (1975). For the period, 1966-1968, Helm obtained slightly better agreement than is seen in Figure 5. In this regard it may be pointed out that Helm plotted the cumulated compaction of 21 different beds of variable thickness while Figure 5 relates to 17 equivalent beds of the same thickness.

Example 4. In the foregoing examples,  $\sigma$  was considered invariant with time. However, there may be cases in which  $\sigma$  is indeed a function of time. One

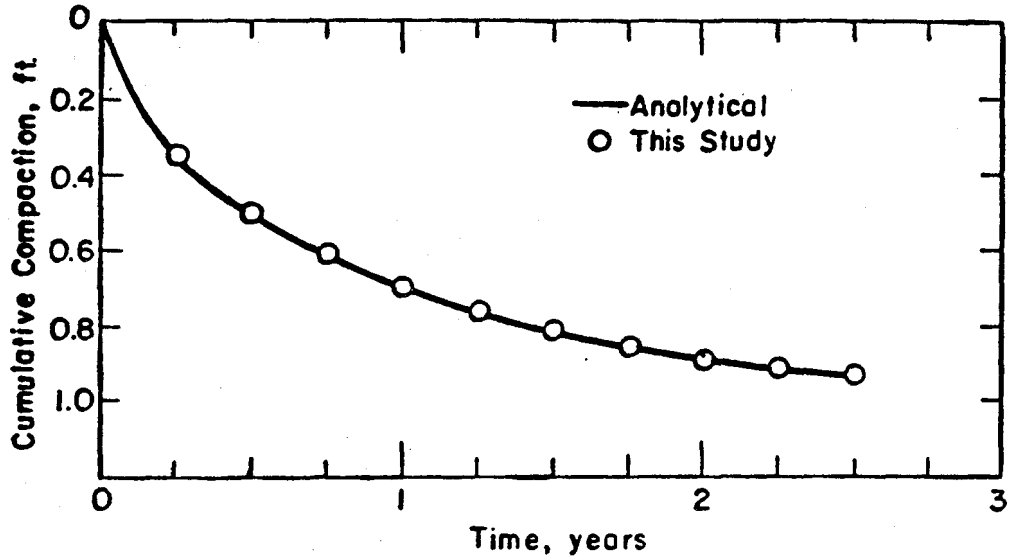
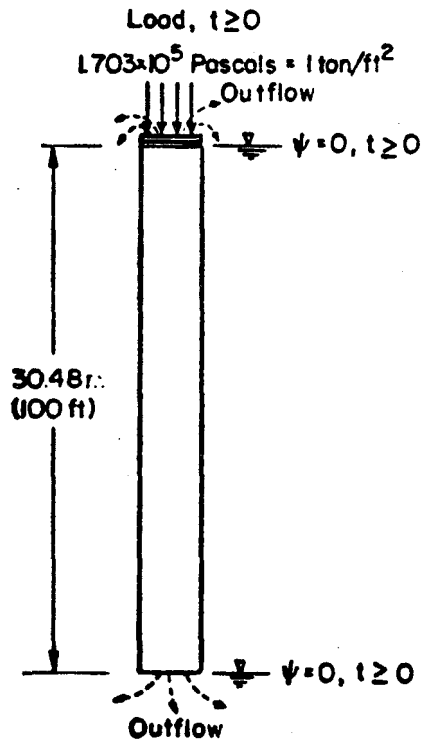


Fig. 1. Compaction of homogeneous clay beds: comparison of analytical and numerical results.



XBL 7612-10869

Fig. 2. Compaction of non homogeneous clay column: initial and boundary conditions.

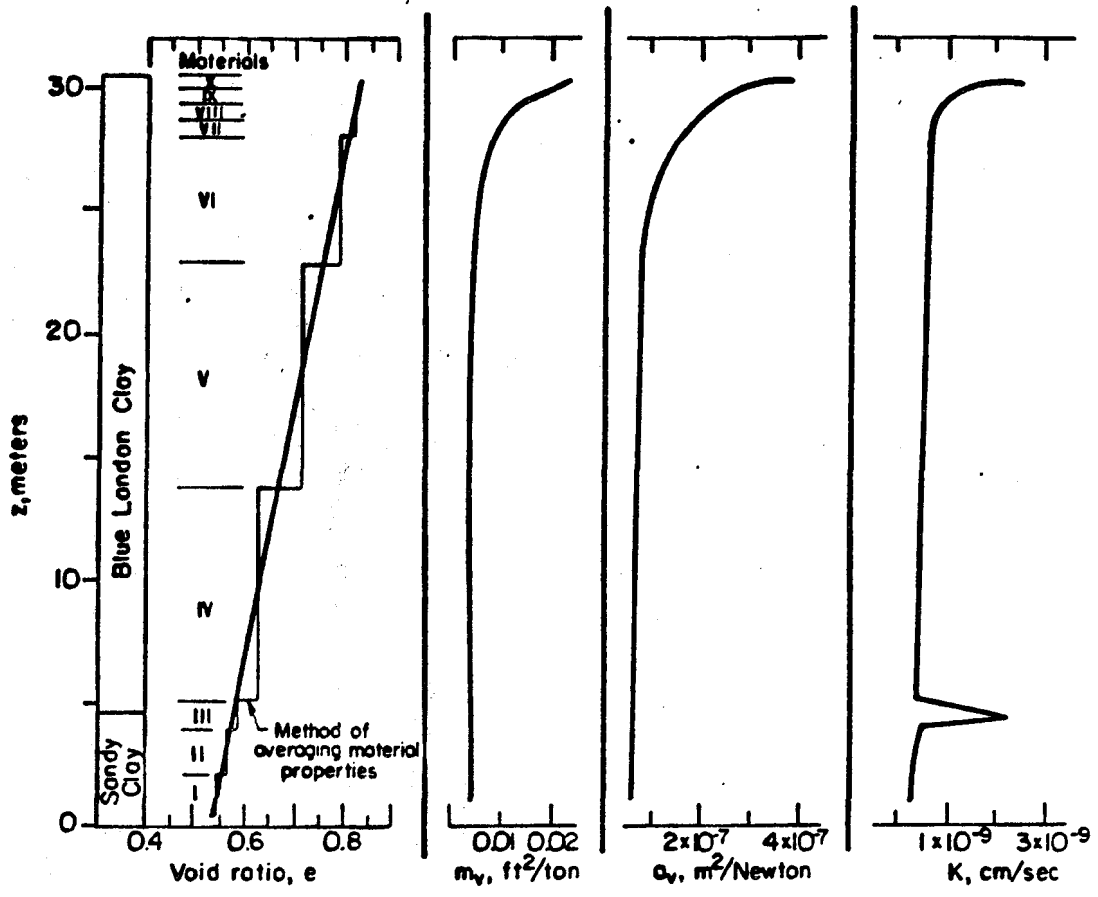
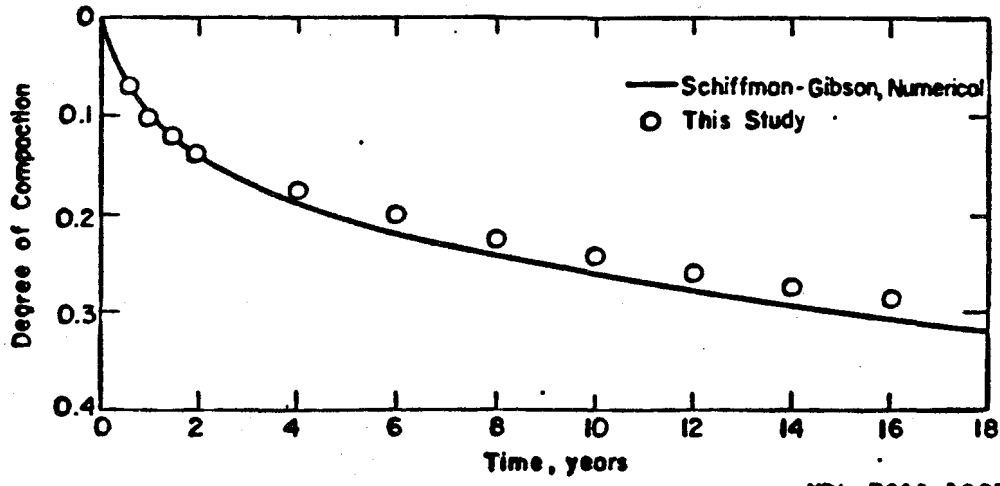
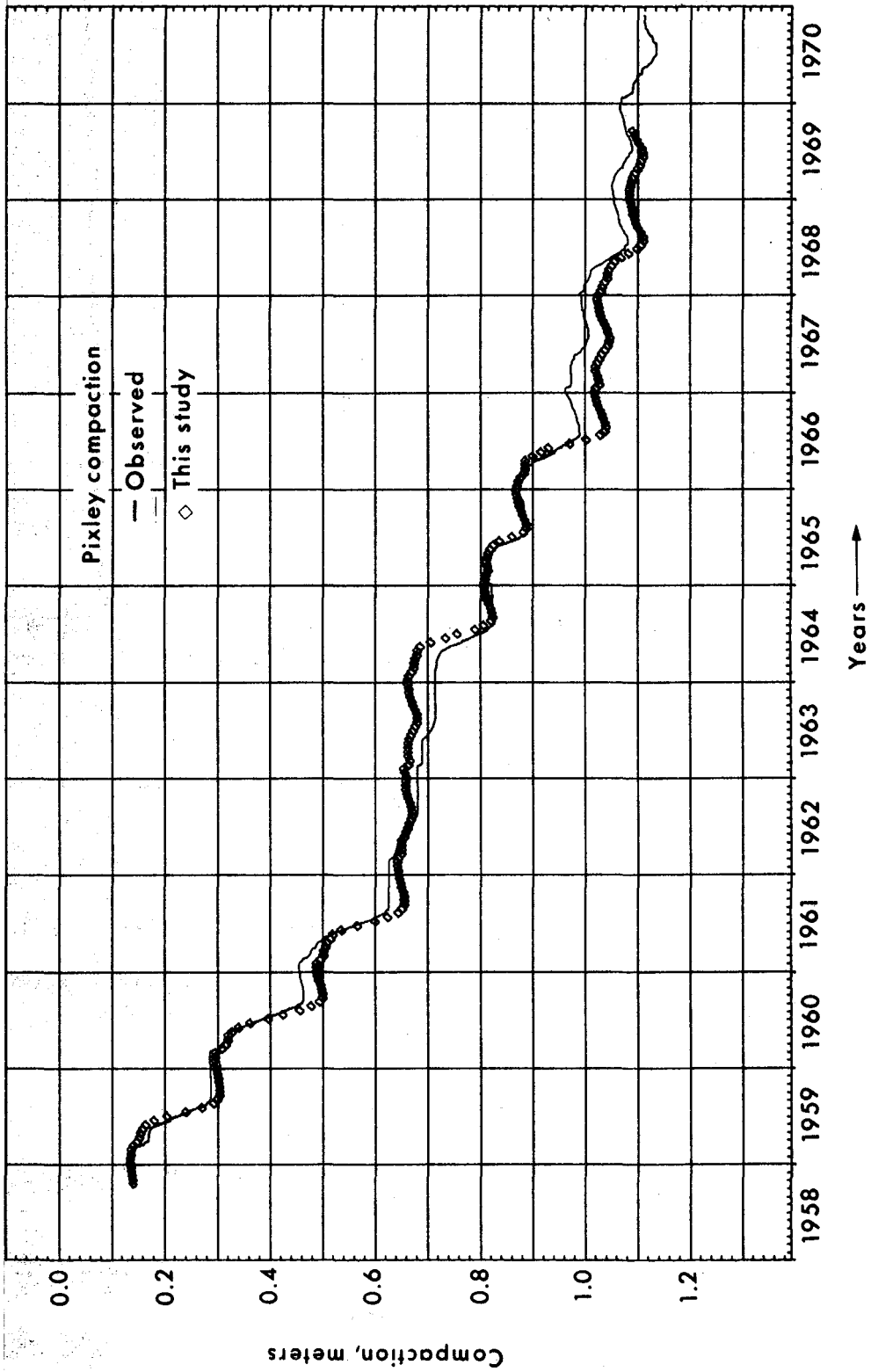


Fig. 3. Compaction of non homogeneous clay column: variation of material properties with depth.



XBL 7612-10872

Fig. 4. Compaction of non homogeneous clay column: comparison of numerical results.



XBL 7612-10874

Fig. 5. Land subsidence at Pixley, California: comparison of observed and computed compactions.

would suspect that in hydrogeological systems the time-scale of such a variation of  $\sigma$  will be very large as compared to that of the drainage phenomenon of interest. To demonstrate how variable total stress could be mathematically modeled, a hypothetical example is chosen from the field of soil mechanics.

A doubly-draining clay layer (Figure 6) is normally consolidated and has  $K' = 9.81 \times 10^{-10}$  m/sec and  $S_s = 5 \times 10^{-3} \text{ m}^{-1}$ . A strip-load,  $10^5 \text{ N/m}^2$ , is gradually applied on a segment of the upper boundary, with the loading being completed after 90 days. It is required to compute compaction during the loading period.

To handle this problem we need to know, a priori, the rate of pore pressure generation caused by the variable load. Note that pore-pressure is generated at constant  $\sigma'$  and compaction takes place only when the generated pore pressure dissipates. Hence, as pore pressure is generated, the total stress is also to be increased by an equal amount.

In this problem, the generation of pore pressure was calculated using the elastic equations (Poulos and Davis, 1974) for uniform strip-loading, assuming that the magnitude of pore pressure generated is equal to the increase in octahedral stress. The ultimate pore pressures so generated are shown contoured in Figure 7. The time-rate of pore pressure generation is equal to the ultimate value divided by the duration of loading. The problem was numerically solved using 280 elements of variable size. The computed compaction profiles at various times are shown in Figure 8.

Example 5. Subsidence caused by withdrawal water by pumping wells is an important field problem. The present mathematical model can, in general, simulate reservoir compaction due to one or more wells producing from a multiple aquifer-aquitard system under arbitrary initial and boundary conditions. For purposes of illustration we consider a simple example.

A one-meter radius well fully penetrates a 20-meter aquifer with  $K = 9.8 \times 10^{-6}$  m/sec and  $S_s = 1 \times 10^{-5}$  (Figure 9) and overlain by 10-meter aquitard with  $K' = 2.9 \times 10^{-10}$  m/sec and  $S_s = 7.54 \times 10^{-4} \text{ m}^{-1}$ . The well produces at a constant rate of  $0.02 \text{ m}^3/\text{sec}$ . It is required to compute the changes in hydraulic head within the system and the compaction as functions of time.

The axisymmetric system was discretized into 421 volume elements with the aquitard divided vertically into 20 zones, each 0.5 m thick. The simulation was carried out for 200 days. Hantush (1960) derived an analytical expression for the drawdown changes within the aquifer in a leaky aquifer system described above. A comparison of the computed results with Hantush's solution is presented in Figure 10, at a point in the aquifer, 125 m away from the well. The computed profiles of compaction are presented in Figure 11. In addition, the computer program also calculates volume strains and strain-rates for each volume element in the system. The contours of equal cumulated strains at the end of 200 days are presented in Figure 12. A mass balance check showed that the volume of water pumped from the aquifer-aquitard system agreed with the total volume change of the system with an error very much less than one percent.

#### Nomenclature

$a_v$	coefficient of compressibility	$[\text{LT}^2/\text{M}]$
$C_c$	compression index	[1]
$C_k$	slope of $e$ versus $\log K$ straight line	[1]
$C_s$	swelling index	[1]
$e$	void ratio	[1]
$G$	mass generation rate from a volume element	[M]
$K, \bar{K}$	hydraulic conductivity; mean hydraulic conductivity	[L/T]
$M_c$	fluid mass capacity	[M/L]

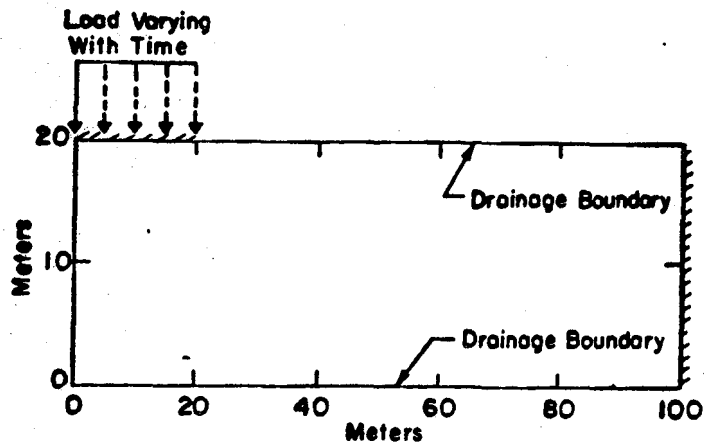


Fig. 6. Compaction due to time-dependent loading: initial and boundary conditions.

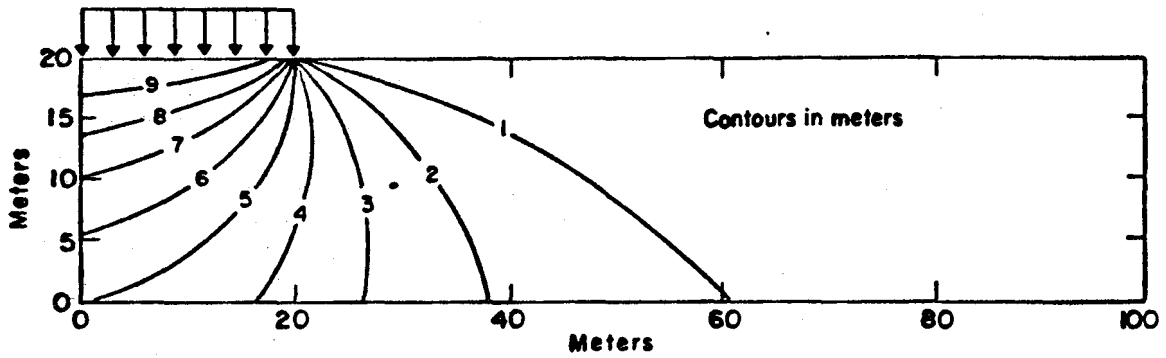


Fig. 7. Compaction due to time-dependent loading: contours of ultimate pore-pressure generated.

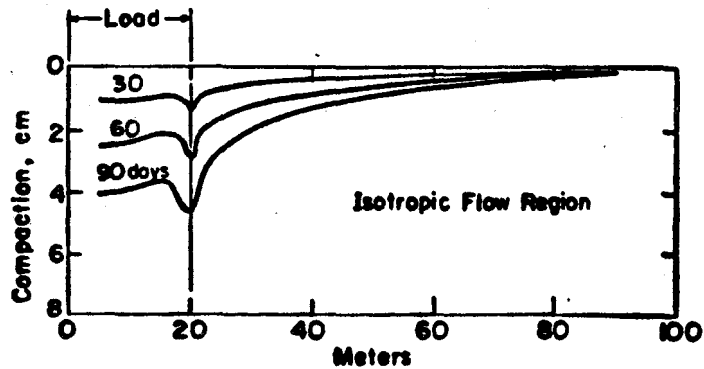


Fig. 8. Compaction due to time-dependent loading: profiles of compaction at different times.

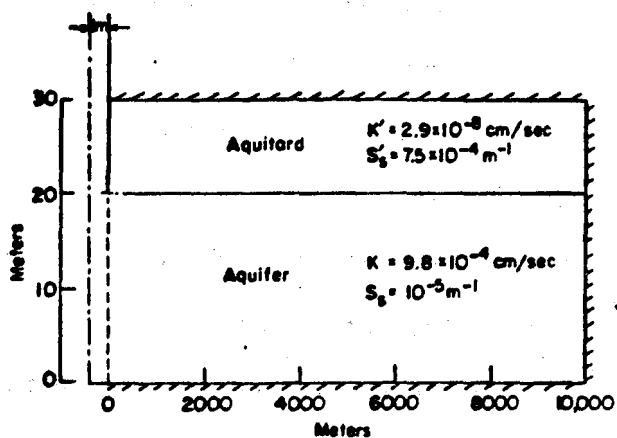


Fig. 9. Leaky aquifer system: boundary conditions.

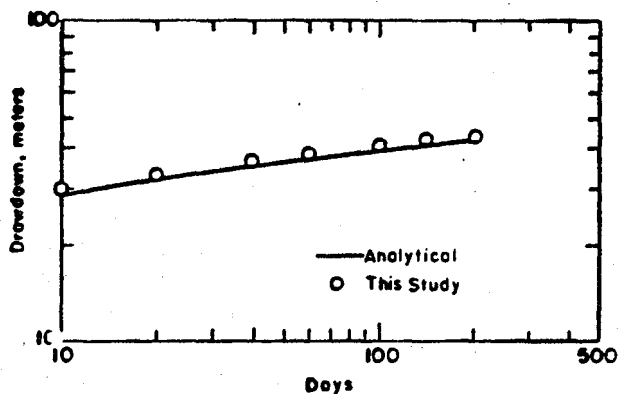


Fig. 10. Leaky aquifer system: comparison of analytical and numerical results at  $r = 125$  m in the aquifer.

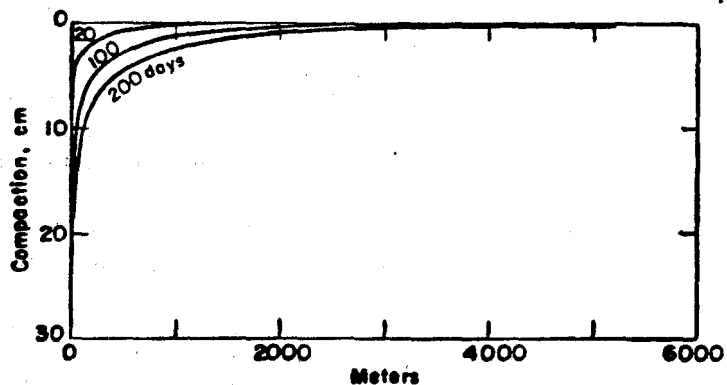


Fig. 11. Leaky aquifer system: profiles of compaction at different times.

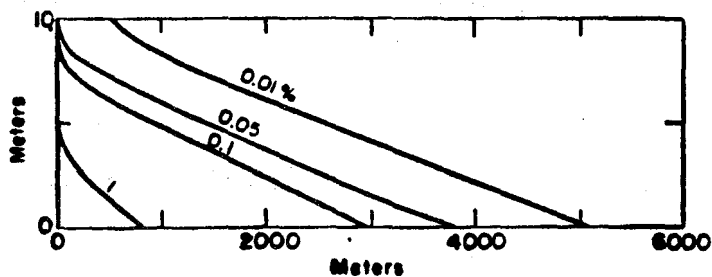


Fig. 12. Leaky aquifer system: contours of equal cumulated strain in the aquitard after 200 days pumping.

$m_v$	coefficient of volumetric compressibility	$[LT^2/M]$
$n$	porosity	$[1]$
$\bar{n}$	unit outer normal	$[1]$
$S$	saturation	$[1]$
$S_s$	coefficient of specific storage	$[1/L]$
$t$	time	$[T]$
$V_s$	volume of solids	$[L^3]$
$V$	bulk volume	$[L^3]$
$z$	elevation above arbitrary datum	$[L]$
$\beta$	compressibility of water	$[LT^2/M]$
$\Gamma$	boundary surface of volume element	$[L^2]$
$\gamma_w$	specific weight of water	$[ML/T^2]$
$\rho_w, \bar{\rho}_w, \rho_{w0}$	density, mean density and reference density of water	$[M/L^3]$
$\sigma$	total stress	$[M/LT^2]$
$\sigma'$	effective stress	$[M/LT^2]$
$\chi'$	coefficient relating pore pressure change to effective stress change	$[1]$
$\psi$	pressure head	$[L]$

### References

- Hantush, M. S., 1960, Modification of the theory of leaky aquifers, J. Geophys. Res., v. 65, no. 11, p. 3713-3726.
- Helm, D. C., 1974, Evaluation of stress-dependent aquitard parameters by simulating observed compaction from known stress history, Ph.D. thesis, Univ. of California, Berkeley, 175 pp.
- Helm, D. C., 1975, One-dimensional simulation of aquifer system compaction near Pixley, California, 1. Constant parameters, Water Resources Res., v. 11, no. 3, p. 465-478.
- Lofgren, B. E. and R. L. Klausning, 1969, Land subsidence due to groundwater withdrawal, Tulare-Wasco area, California, U. S. Geol. Surv. Prof. Paper 437-B, 103 pp.
- Narasimhan, T. N., 1975, A unified numerical model for saturated-unsaturated groundwater flow, Ph.D. thesis, Univ. of Calif., Berkeley, 244 pp.
- Narasimhan, T. N. and P. A. Witherspoon, 1976a, An integrated finite difference method for analyzing fluid flow in porous media, Water Resources Res., v. 12, no. 1, p. 57-64.
- Narasimhan, T. N. and P. A. Witherspoon, 1976b, Numerical model for saturated-unsaturated flow in deformable porous media, Water Resources Res., to be published.
- Poulos, H. G. and E. H. Davis, 1974, Elastic Solutions for Soil and Rock Mechanics, John Wiley and Sons, New York, 411 pp.
- Schiffman, R. L. and R. E. Gibson, 1964, Consolidation of non homogeneous clay layers, Am. Soc. Civil Eng., J. Soil Mech. and Found. Eng., v. 90, no. SM5, p. 1-30.
- Taylor, D. W., 1948, Fundamentals of Soil Mechanics, John Wiley and Sons, New York, 700 pp.

### Acknowledgement

This work was done with support from the U. S. Energy Research and Development Administration.

This report was done with support from the United States Energy Research and Development Administration. Any conclusions or opinions expressed in this report represent solely those of the author(s) and not necessarily those of The Regents of the University of California, the Lawrence Berkeley Laboratory or the United States Energy Research and Development Administration.